Journal of Cerebral Blood Flow & Metabolism (2014) 34, 1887–1897

www.jcbfm.com

ORIGINAL ARTICLE

IGF-1 deficiency impairs cerebral myogenic autoregulation in hypertensive mice

Peter Toth[1,2], Zsuzsanna Tucsek[1], Stefano Tarantini[1], Danuta Sosnowska[1], Tripti Gautam[1], Matthew Mitschelen[1], Akos Koller[2,3], William E Sonntag[1,4], Anna Csiszar[1,2,4] and Zoltan Ungvari[1,2,4]

Aging impairs autoregulatory protection in the brain, exacerbating hypertension-induced cerebromicrovascular injury, neuroinflammation, and development of vascular cognitive impairment. Despite the importance of the age-related decline in circulating insulin-like growth factor-1 (IGF-1) levels in cerebrovascular aging, the effects of IGF-1 deficiency on functional adaptation of cerebral arteries to high blood pressure remain elusive. To determine whether IGF-1 deficiency impairs autoregulatory protection, hypertension was induced in control and IGF-1-deficient mice (*Igf1*$^{f/f}$+TBG-iCre-AAV8) by chronic infusion of angiotensin-II. In hypertensive control mice, cerebral blood flow (CBF) autoregulation was extended to higher pressure values and the pressure-induced tone of middle cerebral arteries (MCAs) was increased. In hypertensive IGF-1-deficient mice, autoregulation was markedly disrupted, and MCAs did not show adaptive increases in myogenic tone. In control mice, the mechanism of adaptation to hypertension involved upregulation of TRPC channels in MCAs and this mechanism was impaired in hypertensive IGF-1-deficient mice. Likely downstream consequences of cerebrovascular autoregulatory dysfunction in hypertensive IGF-1-deficient mice included exacerbated disruption of the blood–brain barrier and neuroinflammation (microglia activation and upregulation of proinflammatory cytokines and chemokines), which were associated with impaired hippocampal cognitive function. Collectively, IGF-1 deficiency impairs autoregulatory protection in the brain of hypertensive mice, potentially exacerbating cerebromicrovascular injury and neuroinflammation mimicking the aging phenotype.

Journal of Cerebral Blood Flow & Metabolism (2014) **34,** 1887–1897; doi:10.1038/jcbfm.2014.156; published online 24 September 2014

Keywords: blood–brain barrier; cerebral blood flow; dementia; neuroinflammation; TRPC; VCI

INTRODUCTION

Pressure-induced myogenic constriction of the cerebral arteries acts as a critical homeostatic mechanism which assures that increased arterial pressure does not penetrate the distal portion of the microcirculation and cause damage to the thin-walled arteriolar and capillary microvessels in the brain.[1,2] In hypertension, the myogenic constriction of cerebral arteries is enhanced and the range of cerebrovascular autoregulation is extended,[3–5] which represent functional adaptation of these vessels to higher systemic blood pressure, protecting the cerebral microcirculation.[1,2,4–6] There is increasing evidence that pathological loss of autoregulatory protection contribute to cerebromicrovascular injury, blood–brain barrier disruption, and intracerebral hemorrhage.[7]

Recent studies suggest that advanced age *per se* is one of the most important factors contributing to dysregulation of myogenic constriction[8,9] and maladaptation of the myogenic machinery to hypertension in the cerebral circulation.[10] Accordingly, recently we have shown that cerebral arteries of aged mice do not exhibit the hypertension-induced adaptive increase in myogenic constriction observed in young mice, due to age-related deficiencies of pressure-induced activation of transient receptor potential canonical type (TRPC) channels.[10,11] Although there is evidence that elderly individuals with hypertension are more likely to develop cerebrovascular pathologies associated with cognitive decline than young individuals,[12,13] the mechanisms by which aging affects the cerebrovasculature are not completely understood. In recent years, an increasing body of evidence has become available suggesting that endocrine mechanisms have an important role in age-related cerebrovascular alterations.[14,15] In particular, the age-related decline in circulating insulin-like growth factor-1 (IGF-1) levels appears to contribute significantly to vascular aging, age-related cerebrovascular changes, and cognitive decline (reviewed recently in ref. 14). Low circulating IGF-1 levels in humans are also associated with an increased risk for hypertension-induced microvascular brain damage[16] and stroke,[17,18] findings that have been also replicated in laboratory animals.[19] There are data available to show that IGF-1 affects the contractile function of the vascular smooth muscle cells[20] and it

[1]Donald W. Reynolds Department of Geriatric Medicine, Reynolds Oklahoma Center on Aging, University of Oklahoma Health Sciences Center, Oklahoma City, Oklahoma, USA; [2]Department of Pathophysiology and Gerontology, Medical School and Szentagothai Research Center, University of Pecs, Pecs, Hungary; [3]Department of Physiology, New York Medical College, Valhalla, New York, USA and [4]The Peggy and Charles Stephenson Cancer Center, University of Oklahoma Health Sciences Center, Oklahoma City, Oklahoma, USA. Correspondence: Professor Z Ungvari, Reynolds Oklahoma Center on Aging, University of Oklahoma Health Sciences Center, 975 NE 10th Street, BRC 1311, Oklahoma City, OK 73104, USA.

E-mail: zoltan-ungvari@ouhsc.edu

This work was supported by grants from the American Heart Association (to PT, ZT, ST, AC and ZU), the Oklahoma Center for the Advancement of Science and Technology (to AC, ZU, WES), the Hungarian National Science Research Fund (OTKA) K 108444 and grants: Developing Competitiveness of Universities in the South Transdanubian Region, 'Identification of new biomarkers..', SROP-4.2.2.A-11/1/KONV-2012-0017 and 'Complex examination of neuropeptide..'SROP-4.2.2.A-11/1/KONV-2012-0024' to AK, the National Center for Complementary and Alternative Medicine (R01-AT006526 to ZU); the National Institute on Aging (R01-AG038747 to WES, R01-NS056218 to AC and WES, 1RO1-AG047879-01 to AC) and the Ellison Medical Foundation (to WES).

Received 13 November 2013; revised 6 August 2014; accepted 9 August 2014; published online 24 September 2014

was shown to improve the autoregulatory function of afferent arterioles in the kidney.[21] Despite these advances, the effects of IGF-1 deficiency on myogenic contraction of cerebral arteries, autoregulation of cerebral blood flow (CBF), and the protective adaptation of cerebral arteries in hypertension remain elusive.

The present study was designed to test the hypotheses that IGF-1 regulates myogenic constriction of cerebral arteries and that low circulating IGF-1 levels impair functional adaptation of these vessels to high blood pressure, mimicking the aging phenotype. A prediction based on this hypothesis is that loss of autoregulatory protection due to IGF-1 deficiency exacerbates hypertension-induced microvascular damage and neuroinflammation leading to cognitive decline. To test our hypotheses, we used a novel mouse model of adult-onset, isolated endocrine IGF-1 deficiency induced by adeno-associated viral knockdown of IGF-1 specifically in the liver of postpubertal mice using Cre-lox technology (*Igf1*$^{f/f}$+TBG-iCre-AAV8).[22] Hypertension was induced in control and IGF-1-deficient mice by chronic infusion of angiotensin II, and changes in arterial myogenic constriction and autoregulation of cerebral blood flow, blood–brain barrier function, markers of neuroinflammation, and cognitive function were assessed.

MATERIALS AND METHODS

All procedures were approved by and followed the guidelines of the Institutional Animal Care and Use Committee of OUHSC in accordance with the ARRIVE guidelines.

Postdevelopmental Liver-Specific Knockdown of *Igf1* in Mice

Male mice homozygous for a floxed exon 4 of the *Igf1* gene (*Igf1*$^{f/f}$) were developed in a mixed 129Sv and C57BL/6 background.[23] These mice have the entirety of exon 4 of the *Igf1* gene flanked by loxP sites, which allows for genomic excision of this exon when exposed to Cre recombinase. Transcripts of the altered *Igf1* gene yield a protein upon translation that fails to bind the IGF receptor. The line was generated in ES cells from 129Sv mice, correctly targeted clones were injected into C57BL/6 blastocysts, and chimeric males were bred to C57BL/6 females. The line at the University of Oklahoma Health Sciences Center (OUHSC) was rederived at Charles River Laboratories in a C57BL/6 background for maintenance of the colony in a specific-pathogen-free rodent barrier facility. Animals were backcrossed to C57BL/6J for six generations and bred to homozygosity. Animals were housed in the Rodent Barrier Facility at OUHSC, on a 12-hour light/12-hour dark cycle, and given access to standard rodent chow (Purina Mills, Richmond, IN, USA) and water *ad libitum*. To provide mice with opportunities for species-specific behaviors basic environmental enrichment was provided (including plastic devices that provide hiding places and opportunity to exercise, and the provision of tissues from which mice readily construct nests).

To target hepatocytes, adeno-associated viruses (AAVs) were purchased from the University of Pennsylvania Vector Core (Philadelphia, PA, USA). At 4 months of age, approximately 1.3×10^{10} viral particles (as assayed by genome content at the University of Pennsylvania) of AAV8.TBG.PI.Cre.rBG or AAV8.TBG.PI.eGFP.WPRE.bGH were administered to *Igf1*$^{f/f}$ mice to knockdown IGF-1 or as a control, respectively. Mice were anesthetized with ketamine/xylazine (100 and 15 mg/kg, respectively), and given intravenous injections of virus diluted to the appropriate concentration in 100 μL 0.9% saline. While AAV8 is effective at transducing multiple tissues after intravenous delivery, including liver, the thyroxine binding globulin (TBG) promoter restricts expression solely to hepatocytes (Supplementary Figure I). Dosages were determined empirically in preliminary studies.

Measurement of Serum Biomarkers

Submandibular venous blood was collected into microcentrifuge tubes using a sterile lancet (Medipoint, Mineola, NY, USA) according to the manufacturer's instructions. Whole blood was centrifuged at 2,500 *g* for 20 minutes at 4°C to collect serum, which was then stored at − 80°C. Serum was processed for ELISA of IGF-1 (R&D Systems, Minneapolis, MN, USA) and γ-glutamyl transferase (Sigma Aldrich, St Louis, MO, USA) according to the manufacturer's protocol. Serum IGF-1 levels are reported in ng/mL. An IGF-1 control sample, with aliquots stored at − 80°C, was included on each plate. IGF binding proteins (IGFBP-1, -2, and -3), adiponectin and insulin were also measured using magnetic bead assays following the manufacturer's guidelines (Milliplex, Billerica, MA, USA).

Infusion of Angiotensin II

To induce hypertension, Alzet mini-osmotic pumps (Model 2006, 0.15 μL/h, 42 days; Durect Co, Cupertino, CA, USA) were implanted into *Igf1*$^{f/f}$+TBG-iCre-AAV8 and control mice (2 months after AAV injection), as previously described.[10] Pumps were filled either with saline vehicle or with solutions of Ang II (Sigma Chemical Co., St Louis, MO, USA) that delivered (subcutaneously) 1,000 ng/min per kilogram of Ang II for 28 days.[10]

Blood Pressure Measurements

Systolic blood pressure of mice in each experimental group was measured by the tail cuff method (CODA Non-Invasive Blood Pressure System, Kent Scientific Co., Torrington, CT, USA) before and 2 weeks (to check for pump failure) and 4 weeks (before the terminal experiments) after the minipump implantation.[10]

Behavioral Studies

On week 4 after implantation, mice were assessed for learning capacity using an elevated plus maze-based learning protocol as previously described.[10] A gray elevated plus maze apparatus was used. Two open arms (25 × 5 cm) and two (25 × 5 cm) closed arms were attached at right angles to a central platform (5 × 5 cm). The apparatus was 40 cm above the floor. Mice were placed individually at the end of an open arm with their back to the central platform. The time for mice to cross a line halfway along one of the closed arms was measured (transfer latency) on day 1 and day 2. Mice had to have their body and each paw on the other side of the line. If a mouse had not crossed the line after 120 seconds, then it was placed beyond it. After crossing the line, mice had 30 seconds for exploring the apparatus. Learning was defined as reduced transfer latency on day 2 compared with day 1. For quantitative analysis, a learning index was calculated based on relative difference in transfer latency on day 1 and day 2. Higher learning index indicates superior hippocampal function.

Cerebrovascular Autoregulation

Cerebrovascular autoregulation was assessed by measuring changes in cortical blood flow as a function of changes in blood pressure, as we previously reported.[10] In brief, on day 28 after implantation animals were anesthetized with α-chloralose (50 mg/kg, intraperitoneally) and urethane (750 mg/kg, intraperitoneally). Previous studies show that in rodents anesthetized with α-chloralose and urethane autoregulation of CBF is preserved, whereas it is compromised after isoflurane anesthesia.[24] The animals were then endotracheally intubated and ventilated (MousVent G500; Kent Scientific Co). Rectal temperature was maintained at 37°C using a thermostatic heating pad (Kent Scientific Co). End-tidal CO_2 was maintained at ~3.7% keeping $PaCO_2$ in the physiologic range (35 to 40 mm Hg). The right femoral artery was cannulated for measurements of the arterial blood pressure (Living Systems Instrumentations, Burlington, VE, USA). Mice were immobilized, placed on a stereotaxic frame, and the scalp and periosteum were pulled aside. Cortical blood flow was measured through the intact skull by laser speckle flowmetry (PeriCam PSI System, Perimed, Stockholm, Sweden) in a region of interest placed between the bregma and lambda. MAP was elevated or decreased in 20-mm Hg steps by intravenous infusion of phenylephrine (1 to 2 μg/kg per minute) or *via* controlled exsanguination (100 to 400 μL of arterial blood), respectively. The range of MAP studied was 40 to 160 mm Hg. Cerebral blood flow values were recorded ~5 minutes after MAP was changed. Changes in CBF were expressed relative to CBF corresponding to a systolic pressure of 80 mm Hg.

Assessment of Pressure- and Flow-Induced Responses in Isolated Middle Cerebral Arteries

On day 28 after implantation, following the *in vivo* measurements, mice were decapitated, the brains were removed and segments of the middle cerebral arteries (MCAs) were isolated using microsurgery instruments for functional studies, as reported.[10] In brief, segments of MCAs were mounted onto two glass micropipettes in an organ chamber and pressurized to 60 mm Hg. The hydrodynamic resistance of the micropipettes was matched. Inflow and outflow pressures were controlled and measured by a pressure servo-control system (Living Systems Instrumentation). Inner

vascular diameter was measured with a custom-built videomicroscope system and continuously recorded using the edge detection function of the Ionoptix Microfluorimeter System (Ionoptix, Milton, MA, USA).[10,11] All vessels were allowed to stabilize for 60 minutes in oxygenated (21% O_2, 5% CO_2, and 75% N_2) Krebs' buffer (composed of (in mmol/L): 110.0 NaCl, 5.0 KCl, 2.5 $CaCl_2$, 1.0 $MgSO_4$, 1.0 KH_2PO_4, 5.5 glucose, and 24.0 $NaHCO_3$, pH ~7.3; at 37°C). The absence of leaks was verified by observing no changes in intraluminal pressure over 3 minutes upon turning off the pressure servo-control system. The presence of an intact endothelium was showed by testing ATP-induced dilation. To test the autoregulatory function of MCAs, both the static and dynamic components in the vascular myogenic response were assessed. The static component in the vascular myogenic response was assessed by measuring changes in vascular diameter in response to stepwise increases (10 mm Hg steps, for 5 to 10 minutes each) in intraluminal pressure (from 0 to 180 mm Hg). The dynamic component in the vascular myogenic response was assessed by measuring the time course of changes in vascular diameter in response to a sudden increase (from 60 to 140 mm Hg) in intraluminal pressure.

To assess flow-induced constriction, which is an important local vasoregulatory mechanism involved in protection of the cerebral microcirculation and regulation of blood flow,[10] the intraluminal flow was increased in isolated MCAs in a stepwise manner by creating a pressure gradient through the vessel (from $\Delta P = 0$ to 40 mm Hg, corresponding to $Q = 0$ to 320 μL/min intraluminal flow) keeping intraluminal pressure constant. Intraluminal flow was measured with a micro-flow meter.

Recent evidence shows that increased activation of a transient receptor potential canonical type (TRPC) channels underlies adaptation of the myogenic machinery to hypertension.[10,11] To assess the role of TRPC channels in changes in myogenic response induced by IGF-1 deficiency and hypertension, the MCAs were incubated with SKF96365 (5×10^{-6} mol/L, for 15 minutes), a potent and specific blocker of TRPC channels, and pressure-induced myogenic constriction was reassessed. 20-hydroxy-5,8,11,14-eicosatetraenoic acid (20-HETE) is a potent vasoconstrictor metabolite of arachidonic acid produced by cytochrome P450 Ω-hydroxylases and has an important role in regulation of TRPC channel activity in cerebral arteries.[10,11] To assess the role of 20-HETE in changes in the myogenic response, MCAs were incubated with the cytochrome P450 ω-hydroxylase inhibitor HET0016 (10^{-6} mol/L, for 30 minutes, purchased from Cayman Chemical Company, Ann Arbor, MI, USA). Then, vascular responses to stepwise increases in intraluminal pressure were reassessed. In additional experiments, vascular dilator capacity was tested by assessing responses to adenosine and ATP (10^{-7} and 10^{-8} mol/L). At the end of each experiment, the passive diameter curves were obtained (0 to 180 mm Hg) in the presence of Ca^{2+}-free Krebs' buffer containing nifedipine (10^{-5} mol/L) to achieve maximal vasodilatation.

Quantitative Real-Time RT-PCR

A quantitative real-time RT-PCR technique was used to analyze mRNA expression of TRPC channels (Supplementary Table I) in MCAs of mice from each experimental group using a Strategen MX3000 platform, as previously reported.[10] In brief, total RNA was isolated with a Mini RNA Isolation Kit (Zymo Research, Orange, CA, USA) and was reverse transcribed using Superscript III RT (Invitrogen).[10,11] Amplification efficiencies were determined using a dilution series of a standard vascular sample. Quantification was performed using the efficiency-corrected ΔΔCq method. The relative quantities of the reference genes *Hprt, Ywhaz, B2m*, and *Actb* were determined and a normalization factor was calculated based on the geometric mean for internal normalization. Fidelity of the PCR was determined by melting temperature analysis and visualization of the product on a 2% agarose gel.

Western Blotting

Immunoblotting studies for TRPC6 in MCA homogenates and for the tight junction proteins (ZO-1, occludin, and claudin-5) in cortical homogenates were performed. In brief, MCAs and cortical samples from each animal ($n = 6$ per experimental group) were homogenized in lysis buffer containing protease inhibitors. Samples were then subjected to SDS-PAGE and transferred onto a PVDF membrane. Membranes were blocked with 5% BSA (in 2% Tween in PBS, for 2 hours, at room temperature), incubated with primary antibody directed against TRPC6 (mouse monoclonal, 1:1,000, overnight at 4°C, Abcam), ZO-1 (clone R40.76 rat monoclonal, 1:500, overnight at 4°C, Millipore), occludin (rabbit polyclonal, 1:1,000; overnight at 4°C, Abcam) or claudin-5 (rabbit polyclonal, 1:1,000, overnight at 4°C, Abcam), and then incubated with the appropriate HRP-conjugated secondary antibodies (for 2 hours, at room temperature). Membranes were developed using Amersham ECL Prime Western Blotting Detection Reagent (GE Healthcare). The relative abundance of studied proteins was determined with densitometry and β-actin (mouse monoclonal, 1:15,000, for 45 minutes, at room temperature, Abcam) as a loading control.

Assessment of the Integrity of the Blood–Brain Barrier

To quantify blood brain barrier (BBB) permeability, we used the sodium fluorescein tracer method, as previously described.[10] In brief, in anesthetized mice the small water-soluble tracer sodium fluorescein (5 mL/kg, 2% in physiologic saline) was administered intravenously by retroorbital injection. After 30 minutes, the animals were transcardially perfused with 1x PBS containing heparin. Then, the mice were decapitated and the brains were removed. From each brain, the hippocampus, the white matter, and the prefrontal cortex were isolated and homogenized. The extravasated sodium fluorescein was quantified spectrophotofluorometrically using a microplate reader and normalized to tissue weight.

Assessment of Inflammatory Gene Expression in the Hippocampus

We analyzed relative abundance of several neuroinflammatory cytokines/chemokines through quantitative real-time PCR with RNA isolated from snap-frozen hippocampal samples. Total RNA was isolated with RNeasy Mini kit (Qiagen) using a fully automated QIAcube-based system. Inflammatory gene expression was assessed using TaqMan Gene Signature real-time PCR arrays (Mouse Immune Array and Alzheimer's Array; Applied Biosystems/Life Technologies, Carlsbad, CA, USA).

Immunofluorescent Labeling and Confocal Microscopy for Microglia Activation

Mice were transcardially perfused with PBS, the brains were removed and hemisected. The left hemispheres were fixed overnight in 4% paraformaldehyde, then they were cryoprotected in a series of graded sucrose solutions (10%, 20%, and 30% overnight), and frozen in Cryo-Gel (Electron Microscopy Sciences, Hatfield, PA, USA). Coronal sections of 70 μm were cut through the hippocampus and stored free-floating in cryopreservative solution (25% glycerol, 25% ethylene glycol, 25% 0.2 M phosphate buffer, 25% distilled water) at − 20°C. Selected sections were ~1.6 mm caudal to Bregma, representing the more rostral hippocampus. After washing (3×5 minutes with TBS plus 3×5 minutes with 1× TBS+0.25% Triton X-100), sections were treated with 1% of sodium-borohydride solution for 5 minutes. After a second washing step (3×5 minutes with distilled water plus 3×5 minutes with 1× TBS) and blocking in 5% BSA/TBS (with 0.5% Triton X-100, 0.3 M glycin and 1% fish gelatin; for 3 hours), sections were immunostained using primary antibodies for 2 nights at 4°C. The following primary antibodies were used: mouse anti-CD31 (1:100, phycoerythrin (PE) conjugated; Cat N: 553373, BD Pharmingen, San Jose CA, USA) or mouse anti-CD31 (1:50, unconjugated; Cat N: 550274, BD Pharmingen) to label endothelial cells, mouse anti-Iba1 (1:50, unconjugated; Cat N: 019-19741, Wako, Richmond, VA, USA) to label microglia and mouse anti-CD68 (1:100, unconjugated; Cat N: ab125212, Abcam, Cambridge, MA, USA) to label activated microglia. The following secondary antibodies were used: goat anti-rabbit IgG, Alexa Fluor 647 (1:1000, Cat N: 4414, Cell Signaling, Danvers, MA, USA) and goat anti-rat IgG, Alexa Fluor 568 (1:1,000, Cat N: A11077, Molecular Probes, Grand Island, NY, USA). Sections were washed for 3×5 minutes with TBS plus 3×5 minutes with 1× TBS+0.25% Triton X-100. For nuclear counterstaining, Hoechst 33342 was used. Then, the sections were transferred to slides and coverslipped. Confocal images were captured using a Leica SP2 MP confocal laser scanning microscope. The total number of Iba1- and CD68-positive activated microglia in the hippocampus was calculated. In each animal, four randomly selected fields from the hippocampus were analyzed in six nonadjacent sections. Six animals per group were analyzed.

Statistical Analysis

Data were analyzed by one-way analysis of variance (ANOVA) followed by Tukey's *post hoc* tests or two-way ANOVA for repeated measures followed by Bonferroni multiple comparison test, as appropriate. All statistical comparisons were performed using Prism 5.0 for Windows (Graphpad Software, La Jolla, CA, USA), and were considered as significant at $P < 0.05$. Data are expressed as mean ± s.e.m. Myogenic tone is calculated as follows: $((D^P\text{-}D^A)/D^P) \times 100$, where D^P is passive diameter (obtained in the absence

of Ca^{2+}) and D^A is active diameter of the vessels at a given intraluminal pressure value.

RESULTS

Circulating Insulin-Like Growth Factor-1 Levels, Other Serum Markers, and Blood Pressure Measurements

Figure 1A shows that mice receiving TBG-iCre-AAV8 had significantly lower serum IGF-1 levels compared with control mice receiving TBG-eGFP-AAV8. Both groups had similar serum IGF-1 levels before administration of liver-targeted viruses.[22] Knockdown of IGF-1 did not lead to change in body weight, serum insulin, IGFBP-1 and -2, adiponectin, and glucose levels (Supplementary Table II). IGFBP3 was decreased in IGF-1-deficient mice, extending previous results obtained in LID mice.[25]

Blood pressure was significantly increased in both control and IGF-1-deficient mice receiving Ang II infusion, as shown in Figure 1B. Although previous studies reported that in mice an ~80% reduction in serum IGF-1 levels may be associated with a ~5 mm Hg increase in blood pressure,[26] in the present study, no significant interaction between IGF-1 levels and blood pressure was noted.

Impaired Cerebrovascular Autoregulation in Insulin-Like Growth Factor-1- Deficient Hypertensive Mice

In control mice, CBF was independent of blood pressure in the range of 60 to 120 mm Hg, which indicates that autoregulation was present (Figures 1 C and 1D). Two-way ANOVA for repeated measures was used to compare profiles of the autoregulation curves. While there was no significant difference between autoregulation in normotensive control mice and IGF-1-deficient mice ($P = 0.47$, Figures 1C and 1D), the autoregulatory curve in the control hypertensive group was significantly different from the autoregulatory curves obtained in the control normotensive group ($P = 0.003$). The Bonferroni multiple comparison test showed that in control hypertensive mice the CBF value corresponding to the 160-mm Hg pressure step was significantly decreased as compared with the respective CBF values obtained in all the other groups (control hypertensive vs. control normotensive $P = 0.01$; control hypertensive vs. IGF-1 deficient $P = 0.017$; control

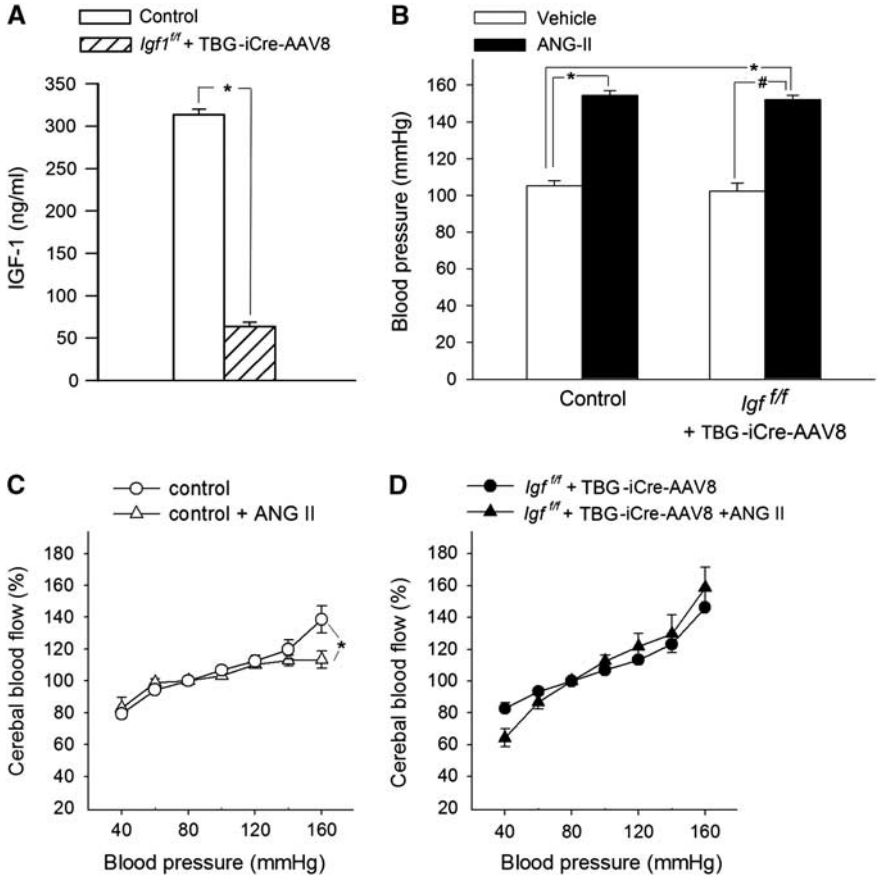

Figure 1. Insulin-like growth factor-1 (IGF-1) deficiency impairs adaptation of cerebrovascular autoregulation to hypertension. (**A**) Serum levels of IGF-1 of control (TBG-eGFP-AAV8) and IGF-1-deficient (TBG-iCre-AAV8) mice after viral injection ($n = 20$ to 25 for each group). In the mouse model used, IGF-1 levels are identical before the injection.[22] (**B**) Effect of chronic infusion of angiotensin II on systolic blood pressure in control and IGF-1-deficient mice. Data are mean ± s.e.m. ($n = 20$ to 25 for each group) $^*P < 0.05$ vs. Control; $^{\#}P < 0.05$ vs. IGF-1 deficient. (**C** and **D**) Relationship between systolic blood pressure and cerebral blood flow (CBF) in normotensive control, hypertensive control (control+Ang II) and normotensive IGF-1-deficient (*Igf1*$^{f/f}$+TBG-iCre-AAV8) and hypertensive IGF-1-deficient mice (*Igf1*$^{f/f}$+TBG-iCre-AAV8+AngII). Data are mean ± s.e.m. ($n = 8$ for each data point). In control mice, CBF is statistically different from the value at 100 mm Hg at pressure values of < 60 and > 140 mm Hg, indicating the autoregulatory range. In control hypertensive mice, there was an expansion of the autoregulated range to high pressure values (**C**), indicating an adaptive response ($^*P < 0.05$ vs. Control at 160 mm Hg), which was completely absent in IGF-1-deficient hypertensive mice (**D**). The blood pressure-CBF curves of normotensive control and normotensive IGF-1-deficient mice did not differ significantly.

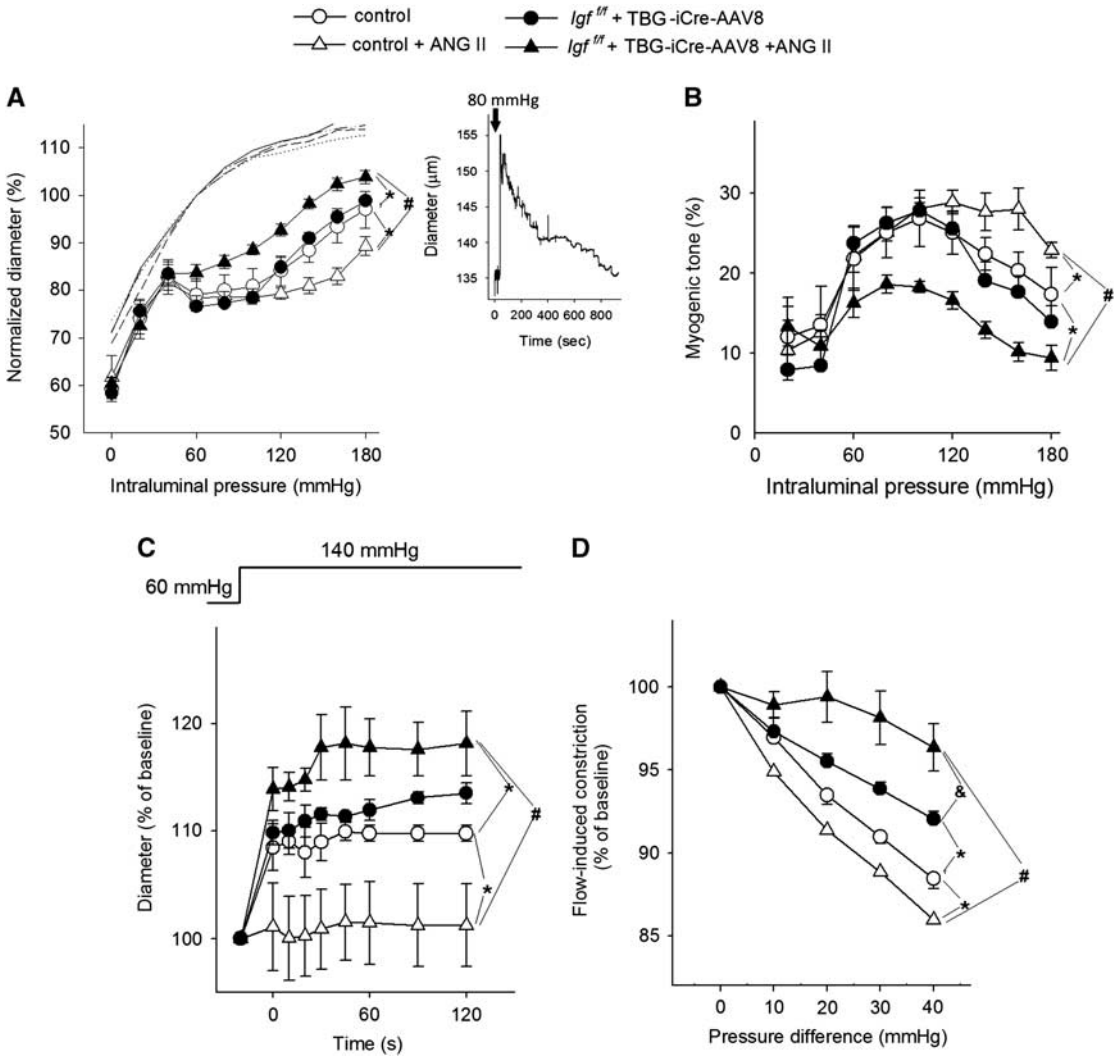

Figure 2. Insulin-like growth factor-1 (IGF-1) deficiency impairs myogenic autoregulation in middle cerebral arteries (MCAs) of hypertensive mice. Panel **A**: Steady-state changes in diameter of MCAs isolated from normotensive control, hypertensive control (control+Ang II) and normotensive IGF-1 deficient (*Igf1*$^{f/f}$+TBG-iCre-AAV8) and hypertensive IGF-1 deficient mice (*Igf1*$^{f/f}$ +TBG-iCre-AAV8+AngII) in response to increases in intraluminal pressure, representing the static component of the myogenic response. Vascular diameters are expressed as percentage of the maximally dilated (passive) diameter of each vessel at 60 mm Hg. Inlet: representative recording showing the time course of changes in diameter of a control MCA in response to an increase in intraluminal pressure (from 60 to 80 mm Hg). Note that an initial dilation is followed by active myogenic constriction. Panel **B** depicts myogenic tone in the studied groups representing the percent change of MCA diameter from the passive diameter in response to a given pressure value. (**C**) Changes in the diameter of MCAs to a sudden increase in intraluminal pressure to 140 mm Hg (from 60 mm Hg), representing the dynamic component of high pressure-induced myogenic response. (**D**) Flow-induced constriction of MCAs (induced by increasing intraluminal flow by creating a pressure gradient through the vessels). Data are mean ± s.e.m. ($n = 8$ to 16). $^{*}P < 0.05$ vs. Control; $^{\#}P < 0.05$ vs. Control+AngII.

hypertensive vs. IGF-1 deficient hypertensive $P < 0.001$). In IGF-1-deficient hypertensive group, the CBF value corresponding to the 160 mm Hg pressure step did not differ from the control normotensive group ($P = 0.26$) and the normotensive IGF-1 deficient group ($P = 0.41$). These findings are consistent with an adaptive expansion of the autoregulated range to high pressure values only in hypertensive control animals (Figure 1C), but not in hypertensive IGF-1 deficient animals (Figure 1D). In IGF-1 deficient hypertensive mice, the essentially linear relationship between blood pressure and CBF at the high pressure range indicates substantial loss of autoregulation (Figure 1D). Resting cortical blood flow was similar in control and IGF-1 deficient mice at 80 mm Hg blood pressure (Supplementary Figure II).

Insulin-like Growth Factor-1 Deficiency Impairs Myogenic Constriction of Cerebral Arteries in Hypertension

Figure 2A shows that myogenic constriction developed in isolated MCAs at intraluminal pressures of 60 to 180 mm Hg. In MCAs of control mice, increases in intravascular pressure induced myogenic constriction at 60 mm Hg, and myogenic tone was maintained at almost the same level to ~130 mm Hg, which overlaps the autoregulatory range of CBF (Figures 2A and 2B,). At higher pressures myogenic constriction tended to decrease and arteries dilate gradually (Figure 2). Myogenic constriction in MCAs from control hypertensive mice was significantly enhanced (vs. control $P < 0.0001$; vs. IGF-1 deficient $P < 0.0001$; $P < 0.0001$ vs. IGF-1

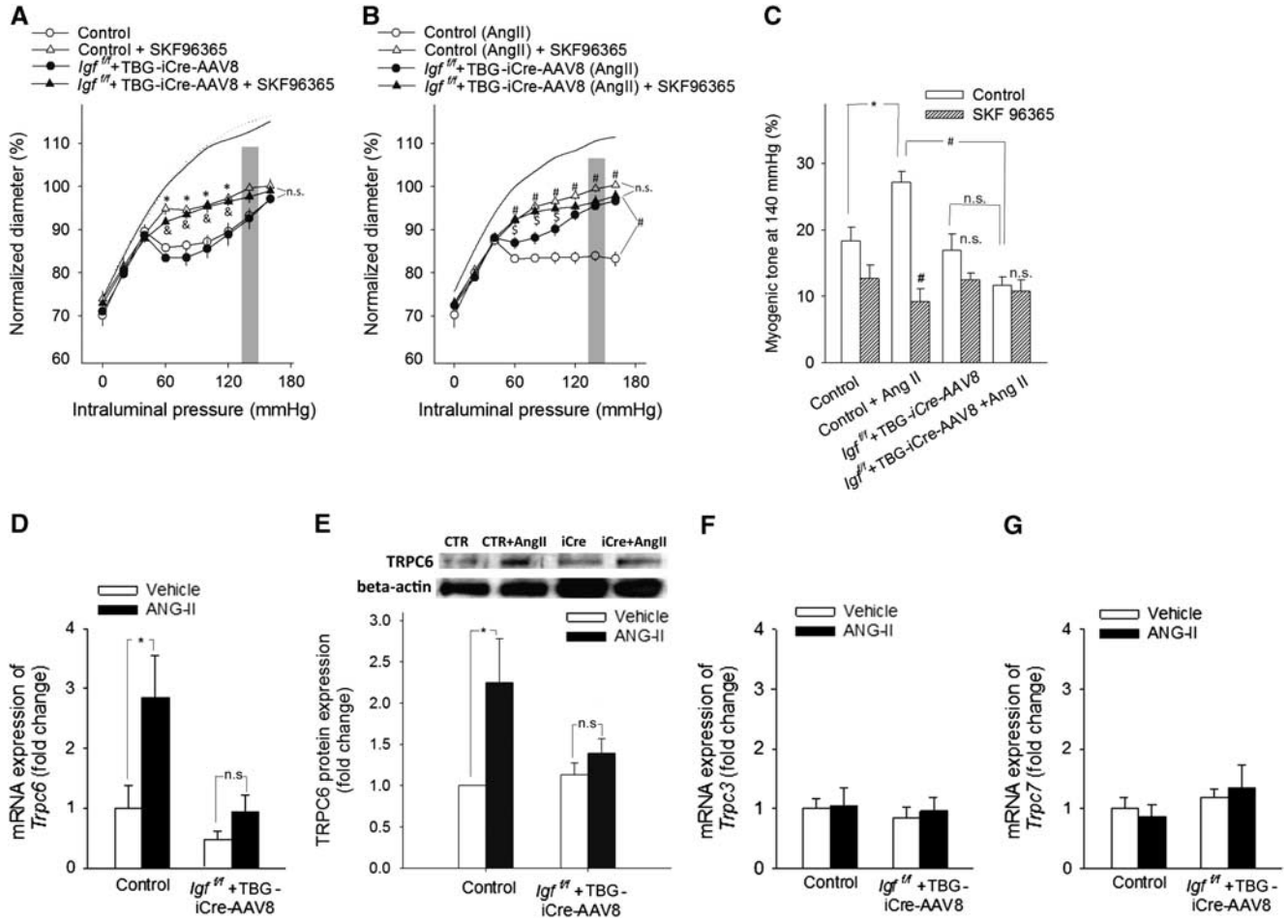

Figure 3. Role of TRPC channels in cerebrovascular autoregulatory dysfunction in hypertensive insulin-like growth factor-1 (IGF-1) deficient mice. Panles **A** and **B**: The effects of SKF96365(5 μmol/L), a TRPC channel blocker on myogenic constriction of middle cerebral arteries (MCAs) isolated from normotensive control, hypertensive control (control+Ang II) and normotensive IGF-1 deficient (*Igf1*$^{f/f}$+TBG-iCre-AAV8) and hypertensive IGF-1 deficient mice (*Igf1*$^{f/f}$+TBG-iCre-AAV8+AngII). Vascular diameters are expressed as percentage of the passive diameter of the vessels at 60 mm Hg. Data are mean ± s.e.m. ($n = 6$ in each group). *$P < 0.05$ vs. Control; #$P < 0.05$ vs. Control+AngII; &$P < 0.05$ vs. IGF-1 deficient; \$$P < 0.05$ vs. IGF-1 deficient+ AngII. (**C**) Myogenic tone of MCAs (in the pressure range highlighted on the myogenic curves on panels A and B) in the absence and presence of SKF96365 at an intraluminal pressure of 140 mm Hg. Note the hypertension-induced, TRPC-dependent extension of myogenic response (myogenic tone) of control animals at high pressure, which is absent in IGF-1 deficient hypertensive mice. Data are mean ± s.e.m. ($n = 6$ in each group). *$P < 0.05$ vs. Control; #$P < 0.05$ vs. Control+AngII. (**D** and **E**) mRNA (**D**; QRT-PCR data) and protein expression (**E**; Western blotting, a representative Western blot (of 6) is presented showing one sample from each group (for each group, $n = 6$ vessels from 6 animals) in MCAs of control and IGF-1 deficient (*Igf1*$^{f/f}$+TBG-iCre-AAV8) mice receiving either vehicle (white bars) or angiotensin II (black bars). (**F** and **G**) panels show the mRNA expression of *TRPC3* and *TRPC7* in MCAs of the same groups of animals. Data are mean ± s.e.m.($n = 6$). *$P < 0.05$ vs. Control; #$P < 0.05$ vs. Control+AngII.

deficient hypertensive $P < 0.0001$) and the myogenic tone was maintained at almost the same level at up to ~ 160 mm Hg, which corresponds to the increased autoregulatory range of CBF in these animals (Figures 2A and 2B,). Middle cerebral arteries of IGF-1 deficient mice did not exhibit a hypertension-induced adaptive increase in myogenic constriction (Figure 2). The myogenic response was significantly decreased in the IGF-1 deficient hypertensive animals compared with both normotensive groups ($P = 0.0001$). The myogenic curves obtained in the two normotensive groups did not differ significantly ($P = 0.42$). The pressure-passive diameter curves were similar in MCAs from each group (Figure 2A). The wall-to-lumen ratio in MCAs is shown in Supplementary Figure IV.

It is an important role of the myogenic mechanism to prevent sudden increases in perfusion pressure in the distal part of microcirculation by increasing arteriolar resistance when pressure increases. Because aging is associated with an impaired dynamic component of the myogenic response,[10] we investigated the time-dependent behavior of the myogenic response as well. The time course of the development of myogenic response significantly differed among the groups. While there was no significant difference between the two normotensive groups ($P = 0.61$), the hypertensive control group significantly differed from the normotensive control group ($P = 0.018$, two-way ANOVA for repeated measures) and the IGF-1 deficient hypertensive group ($P < 0.0001$). In MCAs of control wild type mice a step increase in intraluminal pressure from 60 to 140 mm Hg resulted in slight increase in diameter (Figure 2C). In MCAs of control hypertensive mice the myogenic constriction was enhanced and no increase in diameter was observed. In contrast, MCAs of IGF-1 deficient mice could not maintain resting tone and did not exhibit a

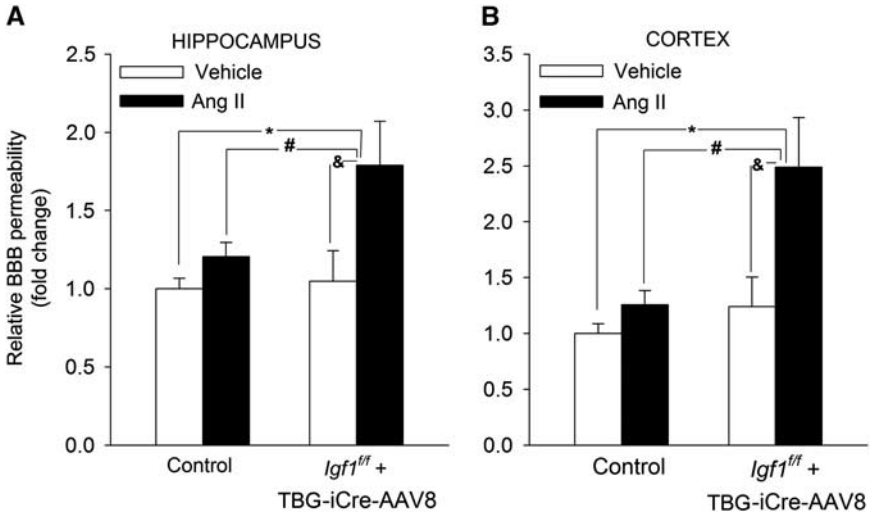

Figure 4. Insulin-like growth factor-1 (IGF-1) deficiency exacerbates hypertension-induced disruption of the blood-brain barrier. Hypertension and IGF-1 deficiency-induced changes in sodium fluorescein content in the hippocampus (**A**) and cortex (**B**) of normotensive control, hypertensive control (control+Ang II) and normotensive IGF-1 deficient (Igf1$^{f/f}$+TBG-iCre-AAV8) and hypertensive IGF-1 deficient mice (Igfq$^{f/f}$ +TBG-iCre-AAV8+AngII). Data are mean ± s.e.m. *$P < 0.05$ vs. Control, $^{\#}P < 0.05$ vs. Control+AngII; $^{\&}P < 0.05$ vs. IGF-1 deficient ($n = 6$ in each group).

hypertension-induced adaptive increase in sudden myogenic constriction (Figure 2C).

Recently it was suggested that in addition to the myogenic response flow-induced constriction of cerebral arteries may also contribute to cerebrovascular autoregulatory function.[27,28] Increases in intraluminal flow elicited vasoconstriction in MCAs of control mice and this response was enhanced by hypertension (control normotensive vs. control hypertensive $P < 0.0001$) (Figure 2D). In contrast, there was no adaptive increase in flow-induced constriction in MCAs of IGF-1 deficient hypertensive mice (Figure 2). In fact, flow-induced constriction decreased in IGF-1 deficient animals (vs control $P < 0.0001$), and further decreased in IGF-1 deficient hypertensive mice (vs. IGF-1 deficient normotensive $P < 0.0001$). Adenosine- and ATP-induced dilations were significantly impaired by hypertension, but IGF-1 deficiency did not have an additional affect (Supplementary Figure V).

Role of TRPC Channels in Functional Maladaptation of Cerebral Arteries to Hypertension in Insulin-like Growth Factor-1 Deficiency

Previous studies showed that TRPC channels mediate myogenic constriction, which are likely activated by pressure-induced 20-HETE synthesis in the vascular wall.[10,11] We found that in MCAs of hypertensive control mice increased myogenic tone was significantly ($P < 0.001$) inhibited by SKF96365 (Figure 3) and HET0016 ($P < 0.001$) (Supplementary Figure III), eliminating the difference between the four groups, extending our recent findings.[10] In contrast, neither SKF96365 (Figures 3A–C) nor HET0016 (Supplementary Figure III) had a significant effect on myogenic constriction of MCAs of hypertensive *Igf1*$^{f/f}$+TBG-iCre-AAV8 mice (for SKF96365 $P = 0.581$; for HET0016 $P = 0.347$). In control experiments, in the absence of the inhibitors repeated assessment of myogenic constriction yielded identical results (control: 79.02 ± 3.3 and 78.9 ± 3.7; *Igf1*$^{f/f}$+TBG-iCre-AAV8: 76.5 ± 2.3 and 75.4 ± 1.9; control+ Ang II: 78.3 ± 1.8 and 78.2 ± 0.9; *Igf1*$^{f/f}$+TBG-iCre-AAV8 +AngII: 83.7 ± 1.8 and 81.3 ± 1.6% of passive diameter at 60 mm Hg for the 1st and 2nd responses, respectively). Hypertension was associated with up-regulated expression of TRPC6 channels ($P = 0.002$) (Figures 3D and 3E) in MCAs of control mice, whereas this adaptive response was significantly impaired or absent in MCAs of *Igf1*$^{f/f}$+TBG-iCre-AAV8 hypertensive mice (vs. IGF-1 deficient $P = 0.4$). In contrast, expression of TRPC3 and TRPC7 channels was unaffected by IGF-1 deficiency and/or hypertension (Figures 3F and 3G).

Insulin-Like Growth Factor-1 Deficiency Exacerbates Hypertension-Induced BBB Disruption and Neuroinflammation

Using a sodium fluorescein tracer assay we tested the hypothesis that cerebrovascular autoregulatory dysfunction in hypertensive *Igf1*$^{f/f}$+TBG-iCre-AAV8 mice is associated with BBB disruption, mimicking the aging phenotype. As predicted by our model, we found that IGF-1 deficiency exacerbates hypertension-induced fluorescein leakage in the hippocampus ($P = 0.036$) and cortex ($P = 0.024$) (Figure 4). IGF-1 deficiency *per se* did not increase the fluorescein leakage either in the cortex or the hippocampi (Figure 4). BBB proteins were unchanged in IGF-1 deficient normotensive mice. Expression of occludin tended to decrease in the brains of hypertensive IGF-1 deficient animals ($P = 0.06$), but due to large variation of data the change fell short of significance (Supplementary Figure VI).

Previous studies suggest that leakage of plasma-derived factors through the damaged BBB has the potential to induce neuroinflammation and compromise higher brain functions.[29] In the present study increased BBB disruption was associated with an increased number of activated perivascular microglia (in IGF-1 deficient hypertensive mice vs. control $P = 0.005$, and vs IGF-1 deficient normotensive mice $P = 0.014$) and upregulation of proinflammatory cytokines and chemokines in the hippocampi of hypertensive *Igf1*$^{f/f}$+TBG-iCre-AAV8 mice (Figure 5 and Supplementary Figure VII, respectively).

Insulin-Like Growth Factor-1 Deficiency Exacerbates Hypertension-Induced Decline in Hippocampal-Dependent Cognitive Function

For normotensive control mice transfer latency on Day 2 was significantly ($P = 0.041$) decreased compared with Day 1, indicating an intact learning effect (learning index: 1; Figure 5E). For hypertensive *Igf1*$^{f/f}$+TBG-iCre-AAV8 mice, transfer latency was similar on Days 1 and 2 ($P = 0.3$) (corresponding to a learning index: ~0), indicating that in these mice IGF-1 deficiency exacerbated hypertension-induced impairment in hippocampal cognitive function (Figure 5E).

DISCUSSION

The results of this study suggest that IGF-1 deficiency is associated with functional maladaptation of cerebral arteries to hypertension, due to, at least in part, the dysregulation of TRP channels. We also show that autoregulatory dysfunction in IGF-1 deficient mice with angiotensin II-induced hypertension is associated with exacerbation of BBB disruption, neuroinflammation and cognitive decline.

Previous studies[1,30] have established that in the cerebral circulation larger pial arteries have a significant role in regulation of cerebrovascular resistance, thus myogenic constriction of

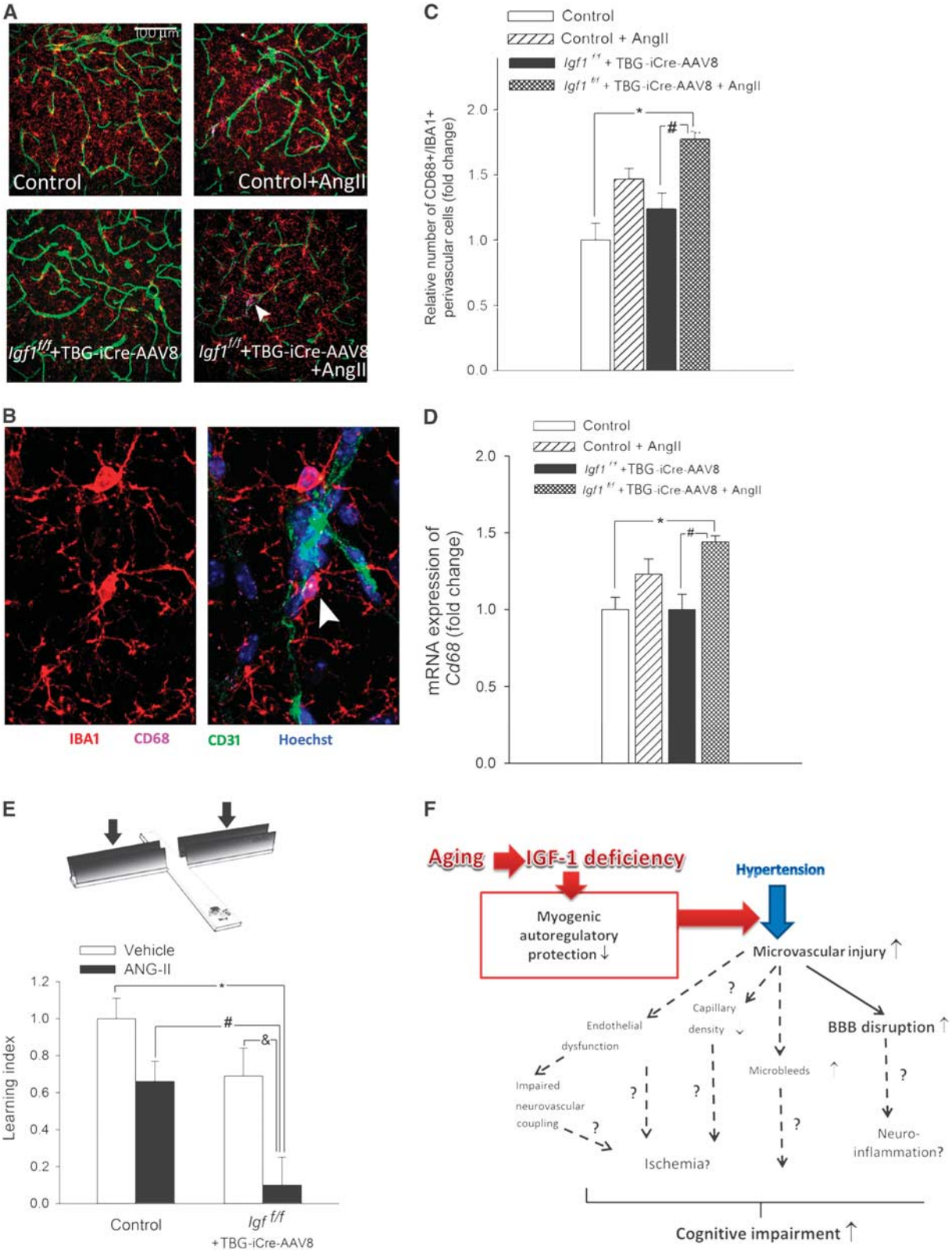

proximal branches of the cerebrovascular tree, including the MCA, is uniquely important for protection of the cerebral microcirculation. There is strong evidence that pressure-induced myogenic constriction of the cerebral arteries in healthy young animals (Figure 2) acts as a critical homeostatic mechanism that assures that increased systemic arterial pressure cannot penetrate the distal portion of the cerebral microcirculation and cause damage to the thin-walled arteriolar and capillary microvessels.[1,2] Here we report that knockdown of hepatic IGF-1 production *per se* does not affect steady-state myogenic constriction in mouse MCAs (Figure 2) and does not alter autoregulation of CBF (Figure 1). Our recent findings suggest that IGF-1 deficiency associated with aging does not alter the static component of the myogenic response in mouse cerebral arteries.[10] Interestingly, IGF-1 deficiency is associated with a mild impairment of both flow-induced constriction and the dynamic component of the myogenic response (Figure 2), suggesting that sudden increases in blood pressure (for example during Valsalva maneuver) may temporarily penetrate the distal portion of the cerebral microcirculation in IGF-1 deficient mice. Further studies are warranted to test this possibility.

Our present study is the first to show that IGF-1 deficiency has a marked negative effect on cerebrovascular adaptation to hypertension. In cerebral arteries isolated from hypertensive control mice[10,11] (Figure 2) and rats [6,31] the myogenic constriction at high pressures is augmented, suggesting that the pressure range for autoregulatory cerebrovascular protection is extended. In addition, in hypertension an enhanced flow-induced constriction (Figure 2) also serves as an adaptive mechanism. The aforementioned functional adaptation of cerebral arteries to higher systemic blood pressure is believed to protect the cerebral microcirculation.[1,2,4–6] Here we provide evidence that cerebral arteries of IGF-1 deficient mice do not exhibit a hypertension-induced adaptive increase in myogenic tone observed in mice with normal IGF-1 levels (Figure 2). Hypertension in IGF-1 deficient mice is also associated with significant impairment of both flow-induced constriction and the dynamic component of the myogenic response (Figure 2). In our recent studies similar maladaptation to hypertension was observed in MCAs of aged mice.[10,11] Both in IGF-1 deficient young mice (Figure 2) and aged mice[10,11] the functional maladaptation of cerebral arteries to hypertension is likely responsible for the loss of autoregulatory protection in the brain observed *in vivo* (Figure 1). In the present study we focused primarily on the upper limit of the autoregulatory range and alterations in the adaptation of the myogenic machinery to high pressure. Further studies are warranted to methodically investigate the effects of hypertension in IGF-1 deficiency on the lower limit of autoregulation of CBF, which has relevance for cerebral ischemia.

Several lines of evidence support the concept that in healthy young mice activation of a TRPC-mediated pathway underlies functional adaptation of cerebral arteries to hypertension[10,11] and that this adaptive response is dysfunctional in mice with IGF-1 deficiency, mimicking the aging phenotype. First, our present findings and results from previous studies show that activation of TRPC channels has an important role in myogenic constriction of cerebral arteries.[32] Second, while in cerebral arteries of young mice angiotensin II-induced hypertension upregulates TRPC6 expression and the TRPC-dependent component of the myogenic constriction (Figure 3), this adaptive response is impaired both in hypertensive IGF-1 deficient mice (Figure 3) and hypertensive aged mice.[10,11] Although SKF 96365 may also inhibit other TRPC channels forming heterotrimeric complex with TRPC6 (TRPC3 and 7), the expression of these channels did not change with hypertension or IGF-1 deficiency (Figure 3). The mechanisms by which IGF-1 promotes TRPC6 expression/activation in hypertensive arteries are presently unknown and may include activation of MAP kinases and/or other cellular signaling pathways. TRPC6 channels are known to be activated by a spectrum of signals (ranging from small second-messenger molecules [e.g. 20-HETE, Supplementary Figure IV.] to physical parameters [lateral-lipid tension]), which modulate their activity during the development of myogenic tone. Further studies are needed to elucidate the regulation of these pathways by IGF-1. In addition, IGF-1 may also directly regulate calcium influx through TRPC channels.[33] Specific activation of TRPC6 channels in response to high intraluminal pressure should be confirmed by future studies using electrophysiological approaches and/or measurement of TRPC6-dependent changes in $[Ca^{2+}]_i$; lack of such measurements is a limitation of our studies. Because flow-induced constriction of cerebral arteries also appears to be predominantly mediated by TRPC channels activated by 20-HETE,[28,34] dysregulation of this pathway in hypertensive *Igf1*$^{f/f}$+TBG-iCre-AAV8 mice is likely to simultaneously impair both the myogenic and the flow-induced components of cerebrovascular autoregulation. Because inhibition of the TRPC channels does not completely abolish myogenic constriction in cerebral arteries of young hypertensive mice, we cannot exclude a potential role for other mechanisms in functional maladaptation to hypertension in IGF-1 deficiency, including pathways involved in cellular calcium homeostasis (e.g. stretch-activation of calcium channels by lipid bilayer stress) in the vascular smooth muscle cells.

Our findings potentially have important clinical significance, as pathological loss of autoregulatory protection likely allows high blood pressure to penetrate the distal, injury-prone portion of the cerebral microcirculation, leading to significant downstream damage. Indeed, epidemiological studies provide evidence that the deleterious cerebrovascular effects of hypertension are exacerbated in elderly patients,[35–37] who exhibit low IGF-1 levels.

Figure 5. Hypertension-induced neuroinflammation and cognitive decline in control and insulin-like growth factor-1 (IGF-1) deficient mice. (**A** and **B**) Confocal images showing perivascular IBA1+/CD68+ activated microglia (arrows; located adjacent to green fluorescent CD31 positive capillaries) in the hippocampus CA-1 region from normotensive control, hypertensive control (control+Ang II) and normotensive IGF-1 deficient (*Igf1*$^{f/f}$+TBG-iCre-AAV8) and hypertensive IGF-1 deficient mice (*Igf1*$^{f/f}$+TBG-iCre-AAV8+AngII). Blue fluorescence: nuclei. Panel **C** depicts summary data of relative changes in the number of perivascular CD68+/IBA1+ positive activated microglia in the hippocampus (fold change). As an additional marker of microglia activation, mRNA expression of *Cd68* was assessed in the hippocampi (Panel **D**). Data are mean ± s.e.m. $^{*}P < 0.05$ vs. normotensive control; $^{\#}P < 0.05$ vs. normotensive IGF-1 deficient. ($n = 6$ in each group). (**E**) IGF-1 deficiency exacerbates hypertension-induced cognitive impairment (elevated plus maze-based learning protocol; see Methods for details). For hypertensive IGF-1 deficient mice, transfer latency was similar on days 1 and 2 (corresponding to a learning index: ~0), indicating that these mice had significantly impaired hippocampal cognitive function. Data are mean ± s.e.m. $^{*}P < 0.05$ vs. Control; $^{\#}P < 0.05$ vs. Control+AngII; $^{\&}P < 0.05$ vs. IGF-1 deficient ($n = 10$ to 12 in each group). (**F**) Proposed scheme depicting the mechanisms by which cerebrovascular autoregulatory dysfunction associated with age-related IGF-1 deficiency exacerbates hypertension-induced microvascular damage and promote the pathogenesis of vascular cognitive impairment (VCI). Future studies should elucidate the mechanistic links (dashed lines; question marks) among endothelial dysfunction, microvascular injury, regional ischemia, microbleeds, neuroinflammation and cognitive impairment.

Here we provide evidence that autoregulatory dysfunction in hypertensive IGF-1 deficient mice is associated with significant BBB disruption (Figure 4). Our recent studies show that autoregulatory dysfunction in mice with age-related IGF-1 deficiency also results in comparable BBB disruption.[10] The mechanisms underlying the exacerbation of hypertension-induced BBB disruption in the aforementioned models are likely multifaceted. In addition to possible changes in endothelial tight junctions future studies should determine the role of changes in astrocytes and pericytes[10] and alterations in the synthesis of components of the extracellular matrix. Increased BBB disruption in hypertensive IGF-1 deficient mice is likely to impair neuronal function by multiple mechanisms,[29] including alterations in the ionic microenvironment around synapses. Another highly important mechanism is the induction of neuroinflammation. Through the damaged BBB plasma constituents enter the brain and have the potential to activate microglia, which confers deleterious neuronal effects. Here we provide evidence that in hypertensive IGF-1 deficient mice BBB disruption is associated with an exacerbated neuroinflammatory response as shown by the increased number of activated perivascular microglia in the hippocampi (Figure 5). We also found that in the hippocampi of hypertensive IGF-1 deficient mice there is an increased expression of inflammatory mediators (Supplementary Figure VII), which are known to be secreted by activated microglia. Microglia-derived proinflammatory cytokines, chemokines and proteases (i.e. MMPs) are thought to have a role in neuronal dysfunction and neurodegeneration in various pathophysiological conditions.[29] To determine whether compromised BBB integrity and chronic low-grade neuroinflammation are sufficient to induce neuronal dysfunction we studied hippocampally dependent learning and memory. Importantly, hypertensive IGF-1 deficient mice exhibited the greatest decline in performance on behavioral tests of hippocampal function (Figure 5), suggesting that exacerbation of neuroinflammation and hypertension-induced neuronal dysfunction in IGF-1 deficient mice may be causally related. Further proof for this concept comes from studies showing that age-related IGF-1 deficiency in rodents is also associated with exacerbation of hypertension-induced microvascular damage, promoting neuroinflammation and cognitive decline. The available human evidence suggest that both IGF-1 deficiency and hypertension compromise higher brain function in humans,[16,38] but further studies are needed to understand their synergistic effects.

CONCLUSIONS AND PERSPECTIVES

In the present study we show that functional adaptation of cerebral arteries to high pressure in angiotensin II-infused IGF-1 deficient mice is impaired and that autoregulatory dysfunction in these animals is associated with BBB disruption and neuroinflammation. Future studies should elucidate the specific IGF-1 -dependent mechanisms that underlie impaired adaptation of cerebral vessels of IGF-1 deficient mice to hypertension, including the signaling pathways involved in transcriptional regulation of TRPC channels. Our findings suggest that in IGF-1 deficient subjects (such as elderly patients and patients with short stature[39,40]) increases in blood pressure are more likely to be transmitted to the thin-walled cerebral microvessels, which likely contributes to the increased prevalence of spontaneous intracerebral hemorrhages observed in these patients.[41] This concept is supported by our recent findings showing increased prevalence of hypertension-induced cerebral microhemorrhages in IGF-1 deficient mice (unpublished data, Toth and Ungvari 2014). Because accumulating evidence supports a role of cerebral microhemorrhages in age-related cognitive decline, future studies should elucidate the causal link among IGF-1 deficiency, cerebrovascular autoregulatory dysfunction and hypertension-induced microhemorrhages as well.

DISCLOSURE/CONFLICT OF INTEREST

The authors declare no conflict of interest.

REFERENCES

1 Kontos HA, Wei EP, Navari RM, Levasseur JE, Rosenblum WI, Patterson JL, Jr. Responses of cerebral arteries and arterioles to acute hypotension and hypertension. *Am J Physiol* 1978; **234**: H371–H383.
2 Harper SL, Bohlen HG. Microvascular adaptation in the cerebral cortex of adult spontaneously hypertensive rats. *Hypertension* 1984; **6**: 408–419.
3 Kontos HA, Wei EP, Raper AJ, Rosenblum WI, Navari RM, Patterson JL, Jr. Role of tissue hypoxia in local regulation of cerebral microcirculation. *Am J Physiol* 1978; **234**: H582–H591.
4 Paulson OB, Strandgaard S, Edvinsson L. Cerebral autoregulation. *Cerebrovasc Brain Metab Rev.* 1990; **2**: 161–192.
5 Strandgaard S, Jones JV, MacKenzie ET, Harper AM. Upper limit of cerebral blood flow autoregulation in experimental renovascular hypertension in the baboon. *Circ Res* 1975; **37**: 164–167.
6 Osol G, Halpern W. Myogenic properties of cerebral blood vessels from normotensive and hypertensive rats. *Am J Physiol* 1985; **249**: H914–H921.
7 Smeda JS. Cerebral vascular changes associated with hemorrhagic stroke in hypertension. *Can J Physiol Pharmacol* 1992; **70**: 552–564.
8 Kang LS, Kim S, Dominguez JM, 2nd, Sindler AL, Dick GM, Muller-Delp JM. Aging and muscle fiber type alter K+ channel contributions to the myogenic response in skeletal muscle arterioles. *J Appl Physiol* 2009; **107**: 389–398.
9 Lott ME, Herr MD, Sinoway LI. Effects of age on brachial artery myogenic responses in humans. *Am J Physiol Regul Integr Comp Physiol* 2004; **287**: R586–R591.
10 Toth P, Tucsek Z, Sosnowska D, Gautam T, Mitschelen M, Tarantini S *et al.* Age-related autoregulatory dysfunction and cerebromicrovascular injury in mice with angiotensin II-induced hypertension. *J Cereb Blood Flow Metab.* 2013; **33**: 1732–1742.
11 Toth P, Csiszar A, Tucsek Z, Sosnowska D, Gautam T, Koller A *et al.* Role of 20-HETE, TRP channels & BKCa in dysregulation of pressure-induced Ca2+ signaling and myogenic constriction of cerebral arteries in aged hypertensive mice. *Am J Physiol Heart Circ Physiol* 2013; **305**: H1698–H1708.
12 Gorelick PB, Scuteri A, Black SE, Decarli C, Greenberg SM, Iadecola C *et al.* Vascular contributions to cognitive impairment and dementia: a statement for healthcare professionals from the American Heart Association/American Stroke Association. *Stroke* 2011; **42**: 2672–2713.
13 Aronow WS, Fleg JL, Pepine CJ, Artinian NT, Bakris G, Brown AS *et al.* ACCF/AHA 2011 expert consensus document on hypertension in the elderly: A report of the american college of cardiology foundation task force on clinical expert consensus documents. *Circulation* 2011; **123**: 2434–2506.
14 Sonntag WE, Deak F, Ashpole N, Toth P, Csiszar A, Freeman W *et al.* Insulin-like growth factor-1 in CNS and cerebrovascular aging. *Front Aging Neurosci* 2013; **5**: 27.
15 Ungvari Z, Csiszar A. The emerging role of IGF-1 deficiency in cardiovascular aging: recent advances. *J Gerontol A Biol Sci Med Sci* 2012; **67**: 599–610.
16 Angelini A, Bendini C, Neviani F, Bergamini L, Manni B, Trenti T *et al.* Insulin-like growth factor-1 (IGF-1): Relation with cognitive functioning and neuroimaging marker of brain damage in a sample of hypertensive elderly subjects. *Arch Gerontol Geriatr* 2009; **49**(Suppl 1):5–12.
17 Johnsen SP, Hundborg HH, Sorensen HT, Orskov H, Tjonneland A, Overvad K *et al.* Insulin-like growth factor (IGF) I, -II, and IGF binding protein-3 and risk of ischemic stroke. *J Clin Endocrinol Metab* 2005; **90**: 5937–5941.
18 Laron Z, Klinger B, Silbergeld A. Patients with Laron syndrome have osteopenia/osteoporosis. *J Bone Miner Res* 1999; **14**: 156–157.
19 Sonntag WE, Carter CS, Ikeno Y, Ekenstedt K, Carlson CS, Loeser RF *et al.* Adult-onset growth hormone and insulin-like growth factor 1 deficiency reduces neoplastic disease, modifies age-related pathology, and increases life span. *Endocrinology* 2005; **146**: 2920–2932.
20 Kobayashi T, Kaneda A, Kamata K. Possible involvement of IGF-1 receptor and IGF-binding protein in insulin-induced enhancement of noradrenaline response in diabetic rat aorta. *Br J Pharmacol* 2003; **140**: 285–294.
21 Lin JJ, Tonshoff B, Bouriquet N, Casellas D, Kaskel FJ, Moore LC. Insulin-like growth factor-1 restores microvascular autoregulation in experimental chronic renal failure. *Kidney Int Suppl* 1998; **67**: S195–S198.
22 Bailey-Downs LC, Mitschelen M, Sosnowska D, Toth P, Pinto JT, Ballabh P *et al.* Liver-specific knockdown of IGF-1 decreases vascular oxidative stress resistance by impairing the Nrf2-dependent antioxidant response: A novel model of vascular aging. *J Gerontol Biol Med Sci* 2012; **67**: 313–329.
23 Liu JL, Grinberg A, Westphal H, Sauer B, Accili D, Karas M *et al.* Insulin-like growth factor-1 affects perinatal lethality and postnatal development in a gene

dosage-dependent manner: Manipulation using the cre/loxp system in transgenic mice. *Mol Endocrinol* 1998; **12**: 1452–1462.
24 Ayata C, Dunn AK, Gursoy OY, Huang Z, Boas DA, Moskowitz MA. Laser speckle flowmetry for the study of cerebrovascular physiology in normal and ischemic mouse cortex. *J Cereb Blood Flow Metab* 2004; **24**: 744–755.
25 Bell RD, Winkler EA, Singh I, Sagare AP, Deane R, Wu Z *et al.* Apolipoprotein E controls cerebrovascular integrity via cyclophilin A. *Nature* 2012; **485**: 512–516.
26 Tivesten A, Bollano E, Andersson I, Fitzgerald S, Caidahl K, Sjogren K *et al.* Liver-derived insulin-like growth factor-1 is involved in the regulation of blood pressure in mice. *Endocrinology* 2002; **143**: 4235–4242.
27 Koller A, Toth P. Contribution of flow-dependent vasomotor mechanisms to the autoregulation of cerebral blood flow. *J Vasc Res* 2012; **49**: 375–389.
28 Toth P, Rozsa B, Springo Z, Doczi T, Koller A. Isolated human and rat cerebral arteries constrict to increases in flow: Role of 20-HETE and TP receptors. *J Cereb Blood Flow Metab* 2011; **31**: 2096–2105.
29 Zlokovic BV. The blood-brain barrier in health and chronic neurodegenerative disorders. *Neuron* 2008; **57**: 178–201.
30 Faraci FM, Heistad DD. Regulation of large cerebral arteries and cerebral microvascular pressure. *Circ Res* 1990; **66**: 8–17.
31 New DI, Chesser AM, Thuraisingham RC, Yaqoob MM. Cerebral artery responses to pressure and flow in uremic hypertensive and spontaneously hypertensive rats. *Am J Physiol Heart Circ Physiol* 2003; **284**: H1212–H1216.
32 Welsh DG, Morielli AD, Nelson MT, Brayden JE. Transient receptor potential channels regulate myogenic tone of resistance arteries. *Circ Res* 2002; **90**: 248–250.
33 Kanzaki M, Zhang YQ, Mashima H, Li L, Shibata H, Kojima I. Translocation of a calcium-permeable cation channel induced by insulin-like growth factor-1. *Nat Cell Biol* 1999; **1**: 165–170.
34 Gebremedhin D, Lange AR, Lowry TF, Taheri MR, Birks EK, Hudetz AG *et al.* Production of 20-HETE and its role in autoregulation of cerebral blood flow. *Circ Res* 2000; **87**: 60–65.
35 Brickman AM, Reitz C, Luchsinger JA, Manly JJ, Schupf N, Muraskin J *et al.* Long-term blood pressure fluctuation and cerebrovascular disease in an elderly cohort. *Arch Neurol* 2010; **67**: 564–569.
36 Reitz C, Tang MX, Manly J, Mayeux R, Luchsinger JA. Hypertension and the risk of mild cognitive impairment. *Arch Neurol* 2007; **64**: 1734–1740.
37 Kuller LH, Lopez OL, Jagust WJ, Becker JT, DeKosky ST, Lyketsos C *et al.* Determinants of vascular dementia in the cardiovascular health cognition study. *Neurology* 2005; **64**: 1548–1552.
38 Bellar D, Glickman EL, Juvancic-Heltzel J, Gunstad J. Serum insulin like growth factor-1 is associated with working memory, executive function and selective attention in a sample of healthy, fit older adults. *Neuroscience* 2011; **178**: 133–137.
39 Goldbourt U, Tanne D. Body height is associated with decreased long-term stroke but not coronary heart disease mortality? *Stroke* 2002; **33**: 743–748.
40 Parker DR, Lapane KL, Lasater TM, Carleton RA. Short stature and cardiovascular disease among men and women from two southeastern new england communities. *Int J Epidemiol* 1998; **27**: 970–975.
41 Poels MM, Ikram MA, van der Lugt A, Hofman A, Krestin GP, Breteler MM *et al.* Incidence of cerebral microbleeds in the general population: The Rotterdam scan study. *Stroke* 2011; **42**: 656–661.

Supplementary Information accompanies the paper on the Journal of Cerebral Blood Flow & Metabolism website (http://www.nature.com/jcbfm)